Title	Elongation Modeling and Compensation for the Flexible Tendon-Sheath System
Author(s)	Sun, ZL; Wang, Z; Phee, SJ
Citation	IEEE/ASME Transactions on Mechatronics, 2014, v. 19, p. 1243-1250
Issued Date	2014
URL	http://hdl.handle.net/10722/209796
Rights	Creative Commons: Attribution 3.0 Hong Kong License ©2014 IEEE. Personal use of this material is permitted. However, permission to reprint/republish this material for advertising or promotional purposes or for creating new collective works for resale or redistribution to servers or lists, or to reuse any copyrighted component of this work in other works must be obtained from the IEEE.

Elongation Modeling and Compensation for the Flexible Tendon–Sheath System

Zhenglong Sun, *Student Member, IEEE*, Zheng Wang, *Member, IEEE*, and Soo Jay Phee, *Member, IEEE*

***Abstract*—In tendon-driven systems, the elongation of the tendon would result in inaccuracy in the position control of the system. This becomes a critical challenge for those applications, such as surgical robots, which require the tendon–sheath system with flexible and even time-varying configurations but lack of corresponding sensory feedback at the distal end due to spatial restrictions. In this paper, we endeavor to address this problem by modeling the tendon elongation in a flexible tendon–sheath system. Targeting at flexibility in practical scenarios, we first derived a model describing the relationship between the overall tendon elongation and the input tension with arbitrary route configurations. It is shown that changes in the route configuration would significantly affect the tendon elongation. We also proposed a remedy to enhance the system tolerance against potential unmodeled perturbations along the transmission route during operation. A scaling factor S was introduced as a design guideline to determine the scaling effect. A dedicated platform that was able to measure the tensions at both ends and the overall tendon elongation was designed and set up to validate the new findings. Discussions were made on the performance and the future implementation of the proposed models and remedy.**

***Index Terms*—Position control, tendon elongation, tendon transmission, tendon–sheath system.**

I. Introduction

TENDON transmission is an active research direction in a robotic manipulator design in order to convey an action at a remote site. It allows the separation of the actuation site and the end effectors without introducing extra components to the end effectors; thus, a lightweight and compact design for the end-effectors could be realized. In addition, the tendons are compliant and flexible, but are able to transmit high power through narrow and even tortuous pathways. Hence, many applications with spatial restrictions often adopt tendon transmission as their actuation mechanism, such as humanoid robotic hands [1]–[4] and wearable exoskeletons for haptic interface [5] and rehabilitation [6], [7]. Most recently, tension transmission has also been applied in applications like rescue robot [8] and even surgical robot for minimally invasive surgery (MIS) [9], [10] and no-scar surgery [11], [12]. The tendon–sheath system (TSS), also known as the cable-conduit system or Bowden cable system, is used to provide the necessary directional guidance in tendon transmission. It allows for simpler mechanical design and less spatial requirements with respect to other solutions based on pulleys or fixed supports. Therefore, the TSS is flexible in adapting to the environment, especially in applications where the work path is concealed or of strict space limitation. For example, through a winding orifice inside the human body [13]. Recent studies have shown that TSS could be a promising solution for surgical systems with success in both animal [14] and human trials [15].

However, the control of these systems could be challenging. Due to the tendon compliance and frictions between the tendon and sheath, the TSS mechanism suffers from significant tension attenuation and motion backlash. These nonlinearities hinder the TSS from being adopted in applications requiring delicate and precise control. Therefore, a proper model for the TSS transmission characteristics is desired to address these nonlinear behaviors, such that effective compensations could be performed to improve the overall system performance. Several activities regarding TSS mechanism modeling were reported in the literature. Many researches focused on the transmission characteristics for the TSS of constant radius [16]–[19]. The assumption of constant radius was valid for their applications in the robotic finger actuation, but limits the generality of the TSS model. Low *et al.* analyzed the TSS with random route configurations by approximating the transmission route configuration with piecewise constant radii [20]. Agrawal *et al.* used discretized model to simulate the transmission characteristics of the TSS in a closed loop [21]. In their works, the TSS modeling is still limited in a pr-defined, fixed tendon–sheath route configuration. Moreover, in-depth discussions of the tension transmission and tendon elongation with respect to the tendon–sheath route configuration, which are the foundations in the control of flexible TSS, are lacking.

Therefore, in order to stretch the limit and extend the transmission model to completely flexible TSS, we have elaborated the tension transmission characteristics of TSS with arbitrary 2-D planar and 3-D spatial configurations in one of our recent publications [22]. However, the tendon elongation problem, as a critical problem for position control in most of the tendon-driven systems, is still lacking attention [23]. For those applications with strict spatial restrictions, where it is difficult to place sensors at the distal end to close the control loop, presence of the tendon elongation could lead to position misalignment and motion backlash. For example, in the application of surgical

Manuscript received September 15, 2012; revised January 23, 2013 and June 11, 2013; accepted July 25, 2013. Date of publication August 29, 2013; date of current version April 25, 2014. Recommended by Technical Editor B. Shirinzadeh. This work was supported by Translational Clinical Research under Grant NMRC/TCR/001-NUS/2007 from the National Medical Research Council of Singapore.

Z. Sun and S. J. Phee are with the School of Mechanical and Aerospace Engineering, Nanyang Technological University, Singapore 639798 (e-mail: sunkurt@gmail.com; MSJPhee@ntu.edu.sg).

Z. Wang is with the School of Engineering and Applied Sciences and the Wyss Institute for Biologically Inspired Engineering, Harvard University, Cambridge, MA 02138 USA (e-mail: zheng.wang@ieee.org).

Color versions of one or more of the figures in this paper are available online at http://ieeexplore.ieee.org.

Digital Object Identifier 10.1109/TMECH.2013.2278613

robots [9], [24], the TSS has to go through narrow and tortuous pathways inside the patient's body; the configuration of the path would be flexible and time-varying throughout the operation. The resulting position errors in the system requires the surgeon to continuously adjust his input commands during the manipulation. Inevitably, it would lower the intuitiveness of the system, and thereafter affect the performance of the surgeon. In order to improve the system performance, in this paper, we will focus on the modeling and compensation of tendon elongation in a flexible TSS with arbitrary route configurations.

II. Modeling Flexible Tendon–Sheath System

In a mechanical remote connection such as TSS, force and position play important roles in the control architecture. In many of the existing works, force or position sensors were placed at the remote robotic end-effectors side, to close the control loop [25], [26]. However, in many applications, no sensory information could be retrieved due to the restrictions such as the workspace constraints. In such cases, a comprehensive modeling of the actuation mechanism is needed to assure the basic requirements in accuracy, then the system could be further benefited from those sophisticated high-level control algorithms, such as real-time identification [27], motion planning [28] and machine learning [29]. Following this train of thought, we present the following investigation on a more generic condition for TSS modeling.

A. Basics for System Position Control Using TSS

For a better understanding of the problem, we start from the analysis of a unidirectional tendon–sheath system. In order to transmit power from one end (proximal) to the other (distal), both ends of the sheath will be immobilized, while the tendon is pulled. The length of tendon that is pulled out from the sheath is accountable for position control. Given a desired user-input position, we must consider the effective elongation to compensate the excess in length. Since the elongation of the tendon is a function of the applied tension, it is essential to understand the tension transmission characteristics along the tendon. In the following section, tension transmission in TSS is first reviewed, followed by modeling of the tendon elongation in flexible TSS. Prior to that, several assumptions regarding flexible TSS and their working conditions are made.

First, as generally accepted in the literature, the loss of tension on the tendon is solely caused by friction between the tendon and the sheath; the elongation of the tendon can only be positive. Second, it is assumed that both tendon and sheath are uniform, so the properties ρ and μ are constant. Finally, to avoid extreme condition, it is assumed that at any time the configuration of TSS will not be completely straightened.

B. Tension Transmission in a Flexible TSS

Consider an infinitesimal segment of tendon and sheath as shown in Fig. 1. Some terminologies not shown in the figure are also explained here. Here, δ is the elongation of the tendon. ζ is the general representation of the direction index, where in

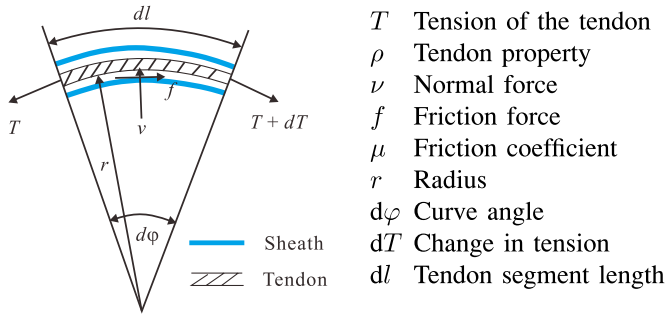

Fig. 1. Small segment of a tendon-sheath system.

case of sliding $\zeta = \mathrm{sgn}\dot{\xi}$, ξ being the displacement of the entire tendon in the sliding case.

From Fig. 1, the basic relations of these variables for an infinitesimal segment could be written as follows:

$$\mathrm{d}l = r\mathrm{d}\varphi, f = \nu\mu, \nu \cong T\mathrm{d}\varphi, \mathrm{d}T = -f\zeta. \tag{1}$$

The change of tendon tension on the segment in study, caused by tendon–sheath friction, can be derived from the basic equation in (1)

$$\frac{\mathrm{d}T}{\mathrm{d}l} = -\frac{\mu}{r}T\zeta = -\mu\kappa T\zeta. \tag{2}$$

In much of the existing literature [16]–[21], the radius r is used to define the shape of the route. It is noted that from this point we use the tendon curvature term κ instead of the radius r, the necessity of such changes would be further explained in the following discussions. The curvature is defined as the reciprocal of the radius

$$\kappa = \frac{1}{r}. \tag{3}$$

It is a property with better physical meaning to define the curve geometry. It describes the magnitude of the variation of the tangent vector in a curve. Following this definition, the curvature of a straight line is zero.

Then, the tension transmission from the proximal end to the distal end of the tendon—sheath could be expressed as

$$T_L = -\int_0^L \mu\zeta\kappa(l)T(l)\,\mathrm{d}l + T_{\mathrm{in}} + T_0 \tag{4}$$

where L is the total length of the tendon, T_{in} is the tension applied to the beginning of the tendon, T_L is the tension transmitted to the end of the tendon, and T_0 is pretension. Note here that both T and κ are functions of l. Therefore, the actual function of the curvature along the tendon $\kappa(l)$ is requested to calculate the integration. However, for general flexible TSS, the curvature is arbitrary, not predefined, and could even be time-varying. Since it is difficult, if not impossible, to measure the radius/curvature of each segment of the tendon–sheath, we proposed a solution in our previous work to remove $\kappa(l)$ from the expression of tension transmission [22].

In [22], we introduce the variable Φ as an accumulated curve angle of the route. It is calculated as the sum of the absolute

value of each infinitesimal curve angle along the TSS

$$\Phi = \sum_{i=1}^{n} |\Phi_i| \tag{5}$$

despite the segments being convex or concave, the sign of all curve segments are considered as positive. n denotes the number of convex and concave segments throughout the length, Φ_i is the curve angle of each curve segment.

Then, by replacing the variable κ using $\mathrm{d}l = r \cdot \mathrm{d}\varphi = 1/\kappa \cdot \mathrm{d}\varphi$, the transmitted tension could be modeled as

$$T_\varphi = \begin{cases} T_{\text{in}} e^{-\mu\varphi\zeta}, & \text{if } \varphi < \Phi_0 \\ T_0, & \text{if } \varphi \geq \Phi_0 \end{cases} \tag{6}$$

where Φ_0 has similar meaning as l_0 which is conventionally used in the literature [16], [17], and [21] to represent the location where the input tension can be effectively transmitted; it represents that in the current shape, the location with maximum accumulated curve angle along the tendon until where the input tension can be effectively transmitted. For any corresponding curve angle $\Phi > \Phi_0$, the tendon segments are considered unchanged. The definition of Φ_0 can be written as a function of input tension T_{in} determined as follows:

$$\Phi_0 = \min\{\varphi | T(\varphi) = T_0\}. \tag{7}$$

In order to derive our elongation model, here the conclusion in our previous publication [22] for the tension transmission of flexible TSS is shown:

Theorem 1: For a flexible TSS with terms defined in (1) and input tension of T_{in}, the tension along each point of the TSS is given by (6).

From *Theorem 1*, we can derive that the tension transmission depends on the accumulated curve angle Φ over the entire tendon. Therefore, as long as no convexity of any segment is affected, and the overall accumulated curve angle is not changed (hence, Φ is not changed), configuration of the TSS will not affect tension transmission. This is important in flexible TSS applications, especially for controlling multi-DoFs robotic manipulator. It implies that the tension transmission characteristics are route configuration independent; and it gives the system more tolerance against small perturbations along the route. Validation experiments and more details could be found in [22].

C. Elongation Model for a Flexible TSS

Understanding the tension transmission characteristics in a flexible TSS, in the following section we continue to propose an elongation model that describe the characteristics of the tendon elongation in a flexible TSS.

For simplicity, we assume the tendon is working within its elastic range. Considering a straight tendon segment with length of l, no tension attenuation occurs since the curvature $\kappa = 0$; therefore, the overall elongation δ is proportional to the tension exerting on it, and can be expressed as

$$\frac{\delta}{l} = \rho T. \tag{8}$$

When the tendon is not straight but of flexible curves, recall the segment of TSS in Fig. 1, the local elongation with corresponding curve angle of φ can be written as

$$\frac{\mathrm{d}\delta(\varphi)}{\mathrm{d}\varphi} = \frac{1}{\kappa}\rho(T(\varphi) - T_0) = \frac{1}{\kappa}\rho T_{\text{in}} e^{-\mu\varphi\zeta} - \frac{1}{\kappa}\rho T_0. \tag{9}$$

Integrating on both sides of (9), with $\delta(0) = 0$, ρ, T_{in}, and T_0 constant, the overall elongation at accumulated curve angle of Φ can be derived

$$\delta_\Phi = \rho T_{\text{in}} \int_0^\Phi \frac{1}{\kappa} e^{-\mu\zeta\varphi}\, \mathrm{d}\varphi - \rho T_0 L. \tag{10}$$

Since the exact function of $\kappa(\varphi)$ is not known, (10) cannot be solved analytically. In order to further investigate into the relation between input tension T_{in} and elongation δ, we divide the tendon into i segments, such that each segment has a constant curvature, denoted as κ_i. Then, it is possible to split the integral correspondingly into i segments, with the lower and upper limit φ_i and φ^i, respectively. Hence, the integral in (10) can be written as the summation of all segments

$$\delta_\Phi = \frac{\rho T_{\text{in}}}{\mu\zeta} \sum_i \frac{1}{\kappa_i}(e^{-\mu\zeta\varphi_i} - e^{-\mu\zeta\varphi^i}) - \rho T_0 L \tag{11}$$

where $\Phi = \sum_i (\varphi^i - \varphi_i)$. Note that if we move the input tension T_{in} into the summation, we can obtain a general expression of tendon elongation

$$\delta_\Phi = \frac{\rho}{\mu\zeta} \sum_i \frac{1}{\kappa_i}(T(\varphi_i) - T(\varphi^i)) - \rho T_0 L. \tag{12}$$

The previous step ensures that each segment i has a constant curvature κ_i. In order to have a better understanding on the relations between the local input tension and curvature, we continue to do the following analysis. Now, consider each one of the i segments, there exist even smaller segments, with a total number of j, such that the curve angle for each of the j segments is the same, denoted by $\bar{\varphi}$. By doing this segmentation, the curvature κ_j values are still constant for each segment, since the new segments are made based on the constant curvature κ_i. Thus, we get a similar expression to (11) with a very important change

$$\delta_\Phi = \frac{\rho}{\mu\zeta}(1 - e^{-\mu\zeta\bar{\varphi}}) \sum_j \frac{T_j}{\kappa_j} - \rho T_0 L \tag{13}$$

where $\Phi = j\bar{\varphi}$, T_j is the input tension at the beginning of each segment. Two observations can be made from (13) about the elongation of flexible TSS.

Remark 1: Elongation is affected by both the curvature configuration and the tension distribution along TSS.

Remark 2: The smaller the κ_j is, the more influence it will have. Thus, the same input tension will result in less elongation at sharp bends than at smoother bends or straight lines.

Based on the tension distribution and transmission model as proposed in *Theorem 1*, we propose a theorem for the tendon elongation of flexible TSS as follows.

Theorem 2: For a flexible TSS with terms defined in (1) and input tension of T_{in}, the overall tendon elongation for TSS with arbitrary route configuration is given by (11).

In *Theorem 2*, relations between the overall tendon elongation δ_Φ and the input tension T_{in} are revealed. In general, the input

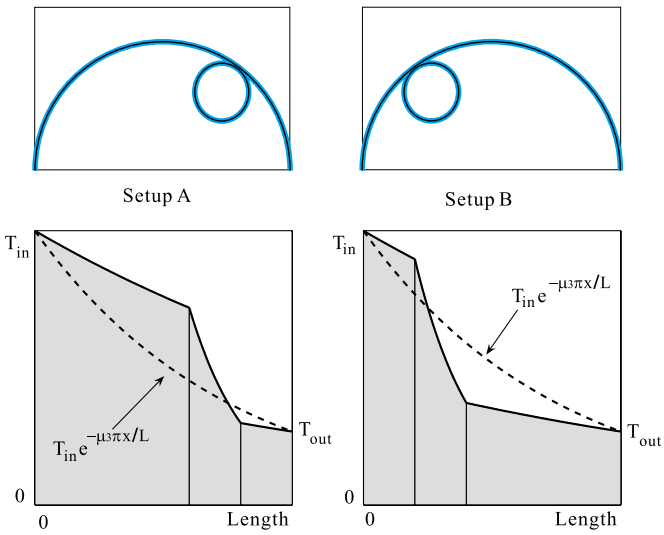

Fig. 2. Illustration of Proposition 1.

tension $T_{\rm in}$ at the proximal end of TSS could be easily measured by using sensors, since there is less strict spatial restrictions. Therefore, once the input tension $T_{\rm in}$ is known, it is desired to restore the tension transmission and tendon elongation through the derived models in *Theorems 1* and *2*. For this purpose, we continue to investigate into the configuration dependence of both the tension transmission and the tendon elongation in TSS; and the following proposition can be made.

Proposition 1 (Configuration Dependence): In TSS, the tension transmission could be route configuration independent, as long as the total accumulated curve angle Φ remains the same. But the elongation appears to be route configuration dependent. The curvature κ of a curve and its location along the TSS would both contribute to the tendon elongation.

Proposition 1 could be illustrated as in Fig. 2. Following the definition in (5), both setups A and B consist of a half circle and a circular loop with a total accumulated curve angle of 3π. The total length and corresponding radii of two curves are identical, while the positions of the loop curve are opposite. As derived in (6), Despite the different route configurations, the tension transmission follows the same relation of $T_{\rm out} = T_{\rm in} e^{-\mu 3\pi}$, as shown in the dotted line. However, tension distribution along the tendon would be different: the closer the curve is to the proximal end, the faster the tension level will drop. In Fig. 2, the tendon elongation could be referred as the areas under the tension distribution curve; and it is obvious that the dimensions of the shaded areas in setups A and B are different.

D. Proposed Method for Elongation Compensation

In practical operations, it is inevitable to encounter perturbations along the route. Here, perturbation refers to the unaware or unmodeled bending curve formed during the transmission. For instance, the tendon–sheath configuration may vary, by alterations due to the carrier platform. It would change the local curvature, and hence the overall curvature distribution. Noted from *Theorem 2* and *Proposition 1*, due to the configuration-dependent nature of the tendon elongation in TSS, such perturbations might affect the overall tendon elongation. Hence, the extent of the system tolerance against such disturbance, becomes critical to the accuracy of the elongation modeling. In the following, we investigated into this issue and proposed a remedy to enhance the system tolerance against unmodeled perturbations.

Recall the equation derived in (13), elongation could be expressed as a summation of the value of local input tension over the corresponding local curvature at each segment. Since the nature of the perturbation, such as curve angle and curvature, are unknown, alternatively, we could reduce their influences to the overall elongation by reducing the local input tension distribution. The local tension could be written as a function of the input tension at the actuator side

$$T_j = T_{\rm in} e^{-\mu\zeta(\bar{\varphi}\cdot j)}. \tag{14}$$

Hence, the closer to the actuator side the curve is, the more influences it will have. Also, it is noted from *Remark 2*, the sharper the bending curve is, the more influences it will have. Based on these criteria, we propose the following remedy: to intentionally introduce a modeled bending curve at the proximal end, close to the actuator side.

In such a manner, the introduced curve could suppress the tendon distribution afterward. Thus, the influences in overall tendon elongation contributed by unmodeled perturbations would be lessened. By controlling the characteristics of the introduced curve, the suppression factor could be adjusted according to different design requirements. In the following, we present a quantitative analysis on this scaling effect.

Recall the expression of tension and elongation in (6) and (10). With an accumulated curve angle of Φ, and no pretension, the transmitted tension and total elongation are

$$T_{\rm out} = T_{\rm in} e^{-\mu\zeta\Phi} \tag{15a}$$

$$\delta_L = \rho T_{\rm in} \int_0^{\Phi} \frac{1}{\kappa(\varphi)} e^{-\mu\zeta\varphi}\, {\rm d}\varphi. \tag{15b}$$

Before we continue with the outcome when perturbation occurs, the following remark is made.

Remark 3: In the TSS, the perturbation might affect at least one or both arguments in the tension and elongation equation: 1) accumulated curve angle Φ and 2) local curve angle/curvature configurations $\kappa(\varphi)$.

In the following, we use $\Delta\Phi$ and $\kappa(\varphi)^*$ as the changes in the accumulated curve angle and local curve angle/curvature configurations caused by perturbations. When a perturbation occurs, corresponding changes in tension and elongation are shown as

$$\Delta T_{\rm out} = T_{\rm in} e^{-\mu\zeta\Phi}(e^{-\mu\zeta\Delta\Phi} - 1) \tag{16a}$$

$$\Delta\delta_L = \rho T_{\rm in}\left(\int_0^{\Phi+\Delta\Phi} \frac{1}{\kappa(\varphi)^*} e^{-\mu\zeta\varphi}\, {\rm d}\varphi - \int_0^{\Phi} \frac{1}{\kappa(\varphi)} e^{-\mu\zeta\varphi}\, {\rm d}\varphi\right). \tag{16b}$$

As a comparison, with the proposed remedy we introduce a curve with curvature of K and angle of β in front, the

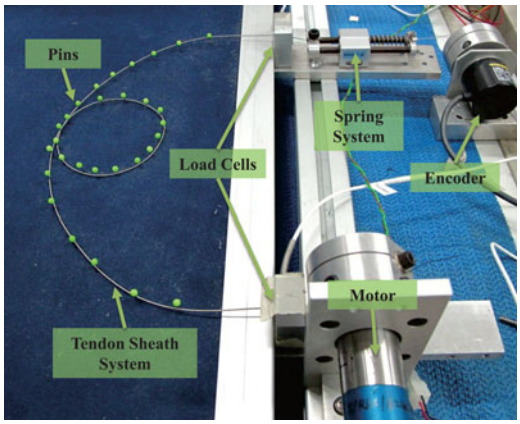

Fig. 3. Experimental setup.

corresponding changes in tension and elongation transmissions under the effect of the same perturbation become

$$\Delta T^*_{\text{out}} = T_{\text{in}} e^{-\mu\zeta(\Phi+\beta)}\left(e^{-\mu\zeta\Delta\Phi} - 1\right) \tag{17a}$$

$$\Delta\delta^*_L = \rho T_{\text{in}}\left(\int_0^{\Phi+\Delta\Phi} \frac{1}{\kappa(\varphi)^*} e^{-\mu\zeta(\beta+\varphi)}\,\mathrm{d}\varphi - \int_0^{\Phi} \frac{1}{\kappa(\varphi)} e^{-\mu\zeta(\beta+\varphi)}\,\mathrm{d}\varphi\right). \tag{17b}$$

Here, we introduce a scaling factor S with an expression of

$$S = e^{-\mu\zeta\beta} \tag{18}$$

and we can find the relations between the changes with and without remedy applied by comparing (16) and (17)

$$\Delta T^*_{\text{out}} = S \cdot \Delta T_{\text{out}}, \quad \Delta\delta^*_L = S \cdot \Delta\delta_L. \tag{19}$$

Based on these findings, we could conclude the following theorem for the proposed remedy:

Theorem 3: By intentionally adding a curve at the proximal end of flexible TSS, the disturbances in tension and elongation caused by unmodeled perturbations could be scaled by a factor of S as shown in (18).

In such a manner, the system would be less sensitive to the changes in the TSS configuration; the system tolerance against unmodeled perturbations is enhanced. Validation results and discussions are made to assess the proposed elongation model and remedy in the following sections.

III. Experimental Validation Results

A. Experimental Setup

An experimental platform was designed to evaluate the overall tendon elongations with respect to the tension inputs, as shown in Fig. 3. In the experiments, we used Teflon coated stainless steel wire rope of 0.54 mm in diameter as tendon and round wire coil with an outer diameter of 0.9 mm and an inner diameter of 0.6 mm as sheath, both were commercial products for industrial applications made by Asahi Intecc, Japan. The tendon–sheath system was placed on a board with adjustable configurations between two fixed bases. A dc servo motor was

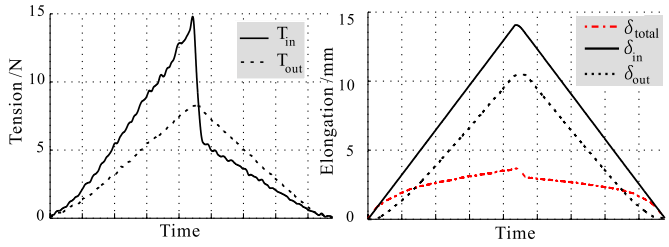

Fig. 4. Tension and elongation over the time for single pull-release cycle.

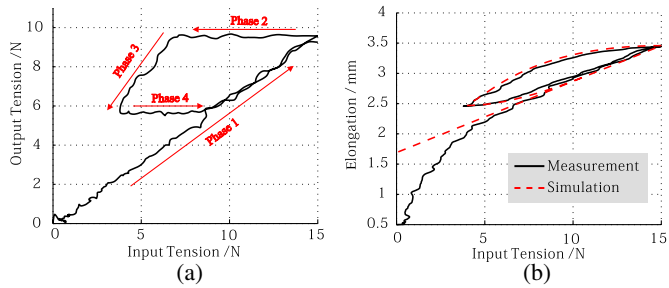

Fig. 5. Tension and elongation characteristics in repeated pull-release cycles. (a) T_{out} versus T_{in}. (b) Elongation versus T_{in}.

used at the proximal end; and a spring system was used at the distal end to ensure the entire tendon would adopt the same direction index ζ in both pulling and releasing phases. Encoders were used to record the displacements of the tendon on both ends. Two washer type load cells (LW1025 from Interface Inc., Atlanta, GA, USA) were placed between two ends and corresponding fixed bases to measure the tensions. The length of the tendon out of the sheath was kept short to minimize its influences on the overall tendon elongation. No pretension T_0 was applied for all the experiments.

B. Validation of the Tendon Elongation Model

The tendon–sheath was arranged in a half-circle configuration with a curve angle of π, and overall length of 50 cm. The motor was actuated in position control mode, pulling the tendon at a constant rate of 0.5 mm/s. When the input tension T_{in} reached 15 N, the actuation direction of the motor was then reversed until the starting position. The experimental result of measured tensions (T_{in} and T_{out}) and elongations (δ_{in} and δ_{out}) over the time is shown in Fig. 4.

It is noted that the input tension T_{in} experiences a significant drop before the output tension T_{out} starts to reduce. Recall the formula (6), the reason for such transition is the sign changing of the direction index ζ. It is known as the dead zone, for direction changing of the tendon displacement at the proximal end to be effectively transmitted to the distal end.

In order to validate the model in describing the elongation characteristics, a repeated pull-release cycle is presented. Maintaining the same configuration, with pretension $T_0 = 0$, the whole actuation process is divided into four distinct phases: 1) Pulling Phase; 2) Pulling to Releasing Phase; 3) Releasing Phase; and 4) Releasing to Pulling Phase as indicated in Fig. 5. The output tension T_{out} and overall elongation δ_L against the input tension T_{in} are shown together in Fig. 5. The tendon

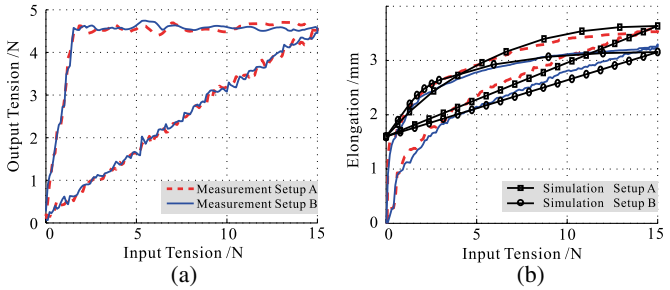

Fig. 6. Experimental measurement and simulation results to validate Proposition 1. (a) T_{out} versus T_{in}. (b) Elongation versus T_{in}.

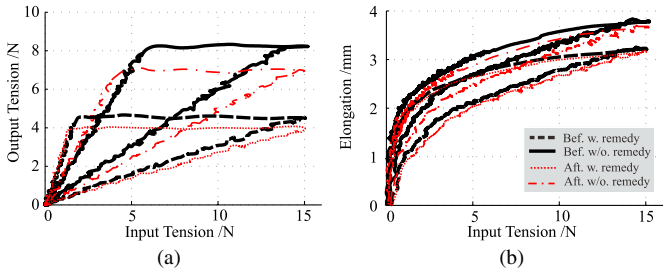

Fig. 7. Effects of the perturbations (before and after) on overall tendon elongation with and without the proposed remedy. (a) T_{out} versus T_{in}. (b) Elongation versus T_{in}.

property was measured prior to the experiment: $\rho = 3.16 \times 10^{-4}$ with an SI unit of N^{-1}. By measuring the tension transmission characteristics, from (6), the friction coefficient was obtained at $\mu = 0.145$. Based on these parameters, simulation results using the proposed model are also plotted in the figure for comparison.

The results show that the simulation is able to predict the actual tendon elongation accurately, for all four phases as defined. However, it is noted that the results show a nonlinear relationship between the overall elongation and the input tension at the beginning. Two possible reasons could be used to explain such observation: 1) as the tendon in the sheath turns from loose to tight, tendon–sheath contact property, in term of the friction coefficient μ, may change and 2) small position realignment might occur in the hardware setup to align the direction with the tension. As a result, the measured tendon elongations have an offset of about 1.69 mm from the simulation results.

Experiments were also performed to validate the *Proposition 1*. The TSS were organized in accordance to the setups A and B as shown in Fig. 2. The experimental measurements and simulations results are plotted in Fig. 6. As anticipated from *Proposition 1*, little difference could be found in the tension transmission. The same total accumulated curve angle Φ resulted in the same T_{out}/T_{in} ratio, in both pulling and releasing phases. However, significant differences could be observed in the tendon elongation. The measured tendon elongation from setup A exceeded the one from setup B by almost 10% (at 0.34 mm). Since the route configuration of the TSS was purposely planned, the exact function of the curvature could then be modeled mathematically. Thus, simulation based on equation (11) derived in *Theorem 2* was carried out. And the simulation results show good consistency with the experimental measurements. Same offset value of 1.69 mm as obtained in previous characteristics validation experiments was used here, to obviate the negative effect due to the nonlinearity at the beginning. To avoid this undesired nonlinearity, it poses necessity for preloading to be applied, which will be discussed further in Section IV-B.

C. Experimental Results With Proposed Remedy

To test the remedy, an intentional defined curve with a curve angle of $\beta = 2\pi$ and a curvature of $K = 40\ m^{-1}$ (radius $r = 25$ mm), was added at the beginning of the configuration. The rest of the configuration remained the same, while the same perturbations were added toward the distal end. Experiments were carried out to compare between results with and without remedy under the effect of perturbations, as shown in Fig. 7.

From the results, it can be noted that the tendon transmissions in both cases have been suppressed. It is noted here that only the pulling phase is of our concern. In order to assess the results, the ratio between the errors in tendon elongation due to perturbations with and without remedy are taken. It is found that the differences between before and after perturbation with remedy are much smaller than the one without (at 15 N, 0.102 mm and 0.256 mm, respectively), with a ratio of about 0.398. Comparing with the scaling factor equation as derived in (18), $S = e^{-\mu\zeta\beta} = 0.402$, it shows that the tendon elongation changes due to the perturbations could be scaled down as predicted with the proposed remedy. Therefore, the overall tendon elongation is less sensitive to the disturbances caused by the perturbation.

IV. Discussion

A. Evaluation of the Tendon Elongation in a TSS

In this paper, we investigated the power transmission model in a flexible TSS, to comply with arbitrary tendon–sheath route configurations, as shown in *Theorems 1* and *2*. Analysis showed that the tension transmission ratio depends only on the total accumulated curve angle Φ of the tendon–sheath route, while the tendon elongation does not only depend on the tensions at two ends, but is also affected by the curvature function $\kappa(\varphi)$ of the route configuration in between. In the proposed elongation model as in (13), the TSS is considered literally *flexible*: there is no restriction on the curvature function, $\kappa(\varphi)$ could be of any function. In addition, different from existing work, where they mainly focus on the tension transmission in the tendon–sheath system [21], [26], such modeling approach could benefit the applications that require flexibility in adapting to any further changes in the configuration. With the elongation model proposed in (13), all the excess curves which are traceable could be updated in the elongation model adaptively.

In a nutshell, the proposed tendon elongation model shows the viability to extend the tendon–sheath mechanism to applications with time-varying flexible configurations. In practice, initial calibration could be performed to obtain the equivalent accumulated total curve angle. Then, based on the changes in the configuration, the elongation model could be updated cor-

respondingly. For example, in robotic endoscopic surgery, the configuration changes of the bending endoscope tip could be monitored and updated in real time [30].

B. Evaluation of the Friction Coefficient

By performing precharacterization to obtain the tendon property ρ, and normal friction coefficient μ, the simulation results based on the proposed model have shown consistency and accuracy in predicting the overall tendon elongation out of the input tension T_{in}. Although the derived model suggests a linear relationship between the elongation and the input tension, a nonlinear response could be observed at the beginning of the loading. This could be due to the complexity of the tribological behavior between the tendon and sheath. In this study, the friction coefficient μ has been assumed to be constant. In order to address this nonlinear behavior at the beginning, considerations over variations in friction coefficient and adhesion conditions of the tendon upon the internal surface of the sheath might be needed.

Such changes in the friction coefficient would be too complex to be modeled. Despite the nonlinear behavior at the beginning, it is noted that for all cases studied in this paper (with and without remedy), the elongation-tension relationship would be in accordance with the simulation results once the input tension T_{in} reached to 4 N. Therefore, it is suggested to apply preloading to avoid the nonlinear effect at the beginning; then the equivalent friction coefficient μ could be assumed to be constant; thereafter, the overall tendon elongation could be predicted by the proposed model in (11).

C. Evaluation of the Proposed Remedy

The effects of the perturbation were examined by experiments. The results showed that without proper constraint, the modeling error caused by perturbations could be quite significant (up to 6.8% without preloading). Therefore, such a disturbance in elongation modeling needs to be addressed.

As suggested in *Theorem 3*, the scaling factor S, could be designed and predetermined. It is affected by the friction coefficient μ, and the curve angle β of the added curve at the beginning. The relation is as shown in Fig. 8. The value of S reduces as the curve angle β increases. And the larger the equivalent average friction coefficient μ is, the more efficient the reduction in S will be. However, this remedy also comes with a cost of sacrificing the tension transmission efficiency. At lower tension transmission rate, there will be higher tension losses. Therefore, the curve angle β and the friction coefficient μ should be selected appropriately. Although the curvature K does not affect the tension transmission, it would contribute to the total tendon elongation. It is to be noted that the curvature K should not be too large. Otherwise it may cause the tendon–sheath contact properties of the added curve to be different from the remaining part; this would violate the assumption of uniform friction coefficient μ throughout the entire length.

In a nutshell, the introduced scaling factor could provide a guideline in determining these parameters when designing the system. Subject to the requirements in the real scenario, we could choose the materials and characteristics of the added curve correspondingly. Although the remedy may change the transmission characteristics, its effects on the tension transmission and tendon elongation could be obtained by precalibration since the introduced curve is predefined and fixed. Thereafter, the models could still be used in the estimation and compensation of the tendon elongation. The purpose of the remedy is to minimize the effect of unknown perturbations. In such a manner, with the derived elongation model and the proposed remedy, the position error caused by tendon elongation could be effectively compensated.

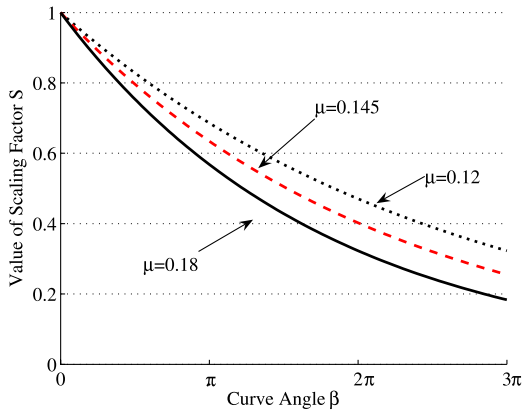

Fig. 8. Ratio of the scaling factor S against curve angle β, with respect to different friction coefficient μ.

V. Conclusion and Future Work

In this paper, we investigated the tendon elongation in a flexible tendon–sheath system. Models for both tension transmission and tendon elongation were proposed and concluded in theorems. In order to analyze the flexibility and time-varying feature of TSS configuration, the concept of accumulated curve angle is used. And it is found that the overall tendon elongation would be affected not only by the accumulated curve angle as the tension transmission, but also by the route configuration of the tendon–sheath, as concluded in Proposition 1. Then, we proposed a remedy by intentionally introducing a curve at the proximal end to enhance the system tolerance against any potential unmodeled perturbations along the route. Guidelines on how to design the added curve were presented in the discussion. Experiments were designed and performed to validate the proposed model and remedy.

This study lays the foundation for achieving accurate position control for any robotic system employing TSS as power transmission. The proposed model requires no sensory feedback from the distal end, but still can provide commensurable estimation accuracy by monitoring the consequential changes in the configuration after the initial calibration. Even in the presence of perturbations, the proposed remedy is still able to suppress the error into a predefined range. It is expected that the promising results could lead advancement in the development of compact and lightweight robotic system in different applications.

REFERENCES

[1] S. Jacobsen, J. Wood, D. Knutti, and K. Biggers, "The utah/mit dextrous hand: Work in progress," *Int. J. Robot. Res.*, vol. 3, no. 4, pp. 21–25, 1984.

[2] J. L. Pons, R. Ceres, and F. Pfeiffer, "Multifingered dextrous robotics hand design and control: A review," *Robotica*, vol. 17, no. 6, pp. 661–674, 1999.

[3] I. M. Sung-yoon Jung and S.-K. Kang, "Design of biomimetic hand prosthesis with tendon-driven five fingers," in *Proc. Int. Conf. Biomed. Rob. Biomech.*, 2008, pp. 895–900.

[4] T. Takaki and T. Omata, "High-performance anthropomorphic robot hand with grasping-force-magnification mechanism," *IEEE/ASME Trans. Mechatronics*, vol. 16, no. 3, pp. 583–591, Jun. 2011.

[5] J. F. Veneman, R. Ekkelenkam, R. Kruidhof, F. C. T. van der Helm, and H. V. D. Kooij, "Design of a series elastic- and bowden-cable-based actuation system for use as torque actuator in exoskeleton-type robots," *Int. J. Robot. Res.*, vol. 25, no. 3, pp. 261–281, 2006.

[6] K. Kong and D. Jeon, "Design and control of an exoskeleton for the elderly and patients," *IEEE/ASME Trans. Mechatronics*, vol. 11, no. 4, pp. 428–432, Aug. 2006.

[7] A. Chiri, N. Vitiello, F. Giovacchini, S. Roccella, F. Vecchi, and M. C. Carrozza, "Mechatronic design and characterization of the index finger module of a hand exoskeleton for post-stroke rehabilitation," *IEEE/ASME Trans. Mechatronics*, vol. 17, no. 5, pp. 884–894, Oct. 2012.

[8] L. Chen, X. Wang, J. Lu, and W. Xu, "Design and preliminary experiments of a robot for searching interior of rubble," in *Proc. Int. Conf. Syst., Man. Cybern.*, 2011, pp. 1956–1961.

[9] D. Abbott, C. Becke, R. Rothstein, and W. Peine, "Design of an endoluminal notes robotic system," in *Proc. Int. Conf. Intel. Rob. Syst.*, 2007, pp. 410–416.

[10] N. Simaan, K. Xu, W. Wei, A. Kapoor, P. Kazanzides, P. Flint, and R. Taylor, "Design and integration of a telerobotic system for minimally invasive surgery of the throat," *Int. J. Robot. Res.*, vol. 28, no. 9, pp. 1134–1153, 2009.

[11] S. Phee, A. Kencana, V. Huynh, Z. Sun, S. Low, K. Yang, D. Lomanto, and K. Ho, "Design of a master and slave transluminal endoscopic robot for natural orifice transluminal endoscopic surgery," *Proc. Inst. Mech. Eng., J. Mech. Eng. Sci.*, vol. 224, no. 7, pp. 1495–1503, 2010.

[12] Z. Sun, R. Y. Ang, E. W. Lim, Z. Wang, K. Y. Ho, and S. J. Phee, "Enhancement of a master-slave robotic system for natural orifice transluminal endoscopic surgery," *Ann. Acad. Med. Singapore*, vol. 40, no. 5, pp. 223–230, 2011.

[13] S. J. Phee, Z. Sun, Z. Wang, J. Y. Y. Wong, and K. Y. Ho, "The future of transluminal surgery," *Expert Rev. Med. Device*, vol. 8, no. 6, pp. 669–671, 2011.

[14] Z. Wang, S. Phee, D. Lomanto, R. Goel, P. Rebala, Z. Sun, S. Trasti, N. Reddy, J. Wong, and K. Y. Ho, "Endoscopic submucosal dissection of gastric lesions by using a master and slave transluminal endoscopic robot: An animal survival study," *Endoscopy*, vol. 44, no. 7, pp. 690–694, 2012.

[15] S. Phee, N. Reddy, P. Chiu, R. Pradeep, G. Rao, Z. Wang, Z. Sun, J. Wong, and K. Y. Ho, "Robot-assisted endoscopic submucosal dissection is effective in treating patients with early-stage gastric neoplasia," *Clin. Gastroenterol Hepa.*, vol. 10, no. 10, pp. 1117–1121, 2012.

[16] M. Kaneko, T. Yamashita, and K. Tanie, "Basic considerations on transmission characteristics for tendon driven robots," in *Proc. Int. Conf. Adv. Robot.*, 1991, pp. 827–832.

[17] G. Palli and C. Melchiorri, "Model and control of tendon-sheath transmission systems," in *Proc. Int. Conf. Robot. Autom.*, 2006, pp. 988–993.

[18] F. Tian and X. Wang, "The design of a tendon-sheath-driven robot," in *Proc. Int. Conf. MMVP*, 2008, pp. 280–284.

[19] L. Chen, X. Wang, and F. Tian, "Tendon-sheath actuated robots and transmission system," in *Proc. Int. Conf. Mechatronics Autom.*, 2009, pp. 3173–3178.

[20] S. J. Phee, S. C. Low, P. Dario, and A. Menciassi, "Tendon sheath analysis for estimation of distal end force and elongation for sensorless distal end," *Robotica*, vol. 28, no. 7, pp. 1073–1082, 2010.

[21] V. Agrawal, W. Peine, and B. Yao, "Modeling of transmission characteristics across a cable-conduit system," *IEEE Trans. Robot.*, vol. 26, no. 5, pp. 914–924, Oct. 2010.

[22] Z. Wang, Z. Sun, and S. Phee, "Modeling tendon-sheath mechanism with flexible configurations for robot control," *Robotica*, to be published, DOI:10.1017/S0263574713000386.

[23] T. Nozaki, T. Mizoguchi, and K. Ohnishi, "Bilateral control method for tendon-driven mechanism considering wire elongation," in *Proc. 38th Annu. Conf. IEEE Ind. Electron. Soc.*, 2012, pp. 2662–2667.

[24] S. Phee, S. Low, V. Huynh, A. Kencana, Z. Sun, and K. Yang, "Master and slave transluminal endoscopic robot (master) for natural orifice transluminal endoscopic surgery (notes)," in *Proc. Int. Conf. IEEE Eng. Med. Bio.*, 2009, pp. 1192–1195.

[25] V. Agrawal, W. Penie, B. Yao, and S. Choi, "Control of cable actuated devices using smooth backlash inverse," in *Proc. Int. Conf. Robot. Autom.*, 2010, pp. 1074–1079.

[26] G. Palli, G. Borghesan, and C. Melchiorri, "Modeling, identification, and control of tendon-based actuation system," *IEEE Trans. Robot.*, vol. 28, no. 2, pp. 277–290, Apr. 2012.

[27] Z. Wang, A. Peer, and M. Buss, "Fast online impedance estimation for robot control," in *Proc. Int. Conf. Mechatronics*, 2009, pp. 1–6.

[28] V. Lippiello, F. Ruggiero, B. Siciliano, and L. Villani, "Visual grasp planning for unknown objects using a multifingered robotic hand," *IEEE/ASME Trans. Mechatronics*, vol. 18, no. 3, pp. 1050–1059, Jun. 2013.

[29] E. Rombokas, M. Malhortra, E. Theodorou, E. Todorov, and Y. Matsuoka, "Reinforcement learning and synergistic control of the act hand," *IEEE/ASME Trans. Mechatronics*, vol. 18, no. 2, pp. 569–577, Apr. 2013.

[30] Z. Wang, Z. Sun, and S. J. Phee, "Haptic feedback and control of a flexible surgical endoscopic robot," *Comp. Meth. Prog. Biomed.*, to be published, DOI: 10.1016/j.cmpb.2013.01.018.

Zhenglong Sun (S'10) received the B.Eng. and M.Eng. degrees from Nanyang Technological University, Singapore. where he is currently working toward the Ph.D degree.

He was at The Johns Hopkins University as a Visiting Scholar in 2008. He is currently working as a Research Fellow at the SUTD-MIT International Design Center. His research interests include haptics feedback, force sensing, surgical robots, and design and development of medical devices.

Zheng Wang (S'08–M'10) received the B.Sc. degree from Tsinghua University, Beijing, China, the M.Sc. degree (with distinction) from Imperial College, London, U.K., and the Ph.D. degree from the Technische Universität München, Munich, Germany.

He was a Postdoctoral Research Fellow at Nanyang Techhnology University, Singapore, between 2010 and 2013. Since early 2013, he has been a Postdoctoral Fellow with joint appointments in the School of Engineering and Applied Sciences and the Wyss Institute of Bioinspired Engineering at Harvard University, Cambridge, MA, USA. His research interests include haptics and compliant human–robot interaction, teleoperation, cable-driven mechanisms, and soft mechanisms.

Soo Jay Phee (M'02) received the B.Eng. (Hons.) and M.Eng. degrees from Nanyang Technological University (NTU), Singapore, in 1996 and 1999, respectively, and the Ph.D. degree from the Scuola Superiore SantAnna, Pisa, Italy, in 2002 on a European Union scholarship.

He is currently an Associate Professor at NTU. He is currently the Head of the Mechatronics and Design Division, School of Mechanical and Aerospace Engineering, NTU. He is the Principal Investigator of a number of interdisciplinary projects. He served as the Program Manager of A*STAR's inaugural MedTech Program. He is also the CEO of EndoMaster Pte Ltd., a company he cofounded to commercialize a surgical robotic system. He has published more than 40 international journal and book chapters. His research interests include medical robotics and mechatronics in medicine.